HHS Public Access

Author manuscript

Virology. Author manuscript; available in PMC 2017 December 01.

Published in final edited form as:

Virology. 2016 December ; 499: 121–135. doi:10.1016/j.virol.2016.09.012.

Mood stabilizers inhibit cytomegalovirus infection

Sara Ornaghi[a,b,c,d], **John N. Davis**[a], **Kelly L. Gorres**[e,1], **George Miller**[e], **Michael J. Paidas**[b], and **Anthony N. van den Pol**[a]

[a]Department of Neurosurgery, Yale University School of Medicine, 333 Cedar Street, 06510, New Haven, Connecticut, USA

[b]Department of Obstetrics, Gynecology, and Reproductive Sciences, Yale University School of Medicine, Yale Women and Children's Center for Blood Disorders and Preeclampsia Advancement, 333 Cedar Street, 06510, New Haven, Connecticut, USA

[c]Department of Surgery and Translational Medicine, PhD program in Neuroscience, University of Milano-Bicocca, via Cadore 48, 20900, Monza, Italy

[d]Department of Obstetrics and Gynecology, Foundation MBBM, University of Milano-Bicocca, via Pergolesi 33, 20900, Monza, Italy

[e]Department of Pediatrics, Yale University School of Medicine, 333 Cedar Street, 06510, New Haven, Connecticut, USA

Abstract

Cytomegalovirus (CMV) infection can generate debilitating disease in immunocompromised individuals and neonates. It is also the most common infectious cause of congenital birth defects in infected fetuses. Available anti-CMV drugs are partially effective but are limited by some toxicity, potential viral resistance, and are not recommended for fetal exposure. Valproate, valpromide, and valnoctamide have been used for many years to treat epilepsy and mood disorders. We report for the first time that, in contrast to the virus-enhancing actions of valproate, valpromide and valnoctamide evoke a substantial and specific inhibition of mouse and human CMV in vitro. In vivo, both drugs safely attenuate mouse CMV, improving survival, body weight, and developmental maturation of infected newborns. The compounds act by a novel mechanism that interferes with CMV attachment to the cell. Our work provides a novel potential direction for CMV therapeutics through repositioning of agents already approved for use in psychiatric disorders.

Address correspondence to Anthony N. van den Pol, anthony.vandenpol@yale.edu.

[1]Present address: Kelly L. Gorres, Department of Chemistry and Biochemistry, University of Wisconsin-La Crosse, La Crosse, WI, USA.

Conflict of interest statement: none.

Keywords

Cytomegalovirus; mood stabilizers; perinatal infection; development

Introduction

Human cytomegalovirus (hCMV) is a common and potentially life-threatening infectious complication in susceptible individuals with immature or compromised immune systems, including neonates, AIDS patients, and transplant recipients. CMV is also the leading viral cause of congenital brain defects, including microcephaly [1–4]. No vaccine is available to prevent CMV infection. Acute and long-term toxicity, carcinogenicity, poor oral bioavailability, and drug resistance significantly limit the use of the current antivirals ganciclovir (GCV), valganciclovir, foscarnet, cidofovir, and fomivirsen [5]; there are no recommended treatments for pregnant mothers and infected fetuses due to the potential teratogenic actions of these compounds [2]. Thus, development of less toxic agents with activity against resistant CMV isolates is needed.

Valproate (VPA) is a widely prescribed anti-epileptic drug employed for the treatment of multiple psychiatric and neurological diseases including bipolar disorder, epilepsy, neuropathic pain, and migraine [6]. VPA is the first-line therapy for pediatric epilepsy [7]. Significant side effects of VPA administration include liver toxicity and teratogenesis [7, 8]. A free carboxylic group in the chemical structure and an inhibitory action on histone deacetylase (HDAC) underlie the detrimental effects exerted by VPA on fetal development and can lead to neural tube defects, skeletal abnormalities, and autism [9–15].

Valpromide (VPD), a more effective and less toxic anti-epileptic homologue of VPA, has been used as a mood stabilizer in bipolar disorder for over 25 years [16]. In contrast to VPA, VPD lacks the free carboxylic group and the HDAC inhibitory activity and therefore the related teratogenic risk, as demonstrated in a number of animal models [10, 11, 17].

Although both VPA and VPD attenuate reactivation from latency of Epstein Barr virus [18], VPA enhances the infectivity and replication of a large variety of other viruses including HIV [19], vesicular stomatitis virus (VSV) [20], Kaposi’s sarcoma-associated herpes virus [21], herpes simplex viruses [22, 23], human herpes virus 6 [24], and hCMV [25–27] through a mechanism involving HDAC inhibition. These virus-enhancing effects are exerted at doses therapeutic for anti-epileptic and mood stabilizing purposes [28–30], thus raising concerns over the use of VPA in congenitally CMV-infected neonates experiencing seizures and in AIDS patients with CMV- and HIV-mediated neurological disorders [31]. Given the absence of HDAC inhibition, we hypothesized that VPD might show a reduced enhancement of CMV infection compared with VPA.

Materials and Methods

Cells

NIH/3T3 (CRL-1658) and Vero (CCL-81) cells were purchased from the American Type Culture Collection (ATCC) (Manassas, VA), normal human dermal fibroblasts (HDF) were

obtained from Cambrex (Walkersville, MD), Neuro-2a (CCL-131) were kindly provided by A. Bordey (Yale University, New Haven, CT), and U-373 MG cells were a gift from R. Matthews (Syracuse, NY). Vero cells were grown and maintained in Eagle's Minimum Essential Medium (MEM) supplemented with 10% fetal bovine serum (FBS) and 1% pen/strep (Invitrogen, Carlsbad, CA). All the other cell lines were maintained in Dulbecco's modified Eagle's essential medium (DMEM) supplemented with 10% FBS and 1% pen/strep. Primary cultures of mouse glia were established using whole brain tissue harvested from P5 mice and maintained in DMEM [32]. All cultures were kept in a humified atmosphere containing 5% CO_2 at 37°C.

Viruses

A brief description of each virus used is given below.

mCMV-GFP

Recombinant murine CMV (mCMV, MC.55) expressing enhanced green fluorescent protein (EGFP) was derived from the K181 strain. The expression cassette containing the EGFP gene controlled by the human elongation factor 1 alpha (EF1-alpha) promoter was inserted into the immediate early gene (IE-2) site. NIH/3T3 cells were used for viral propagation and titering by plaque assay [32].

hCMV-GFP

Recombinant hCMV expressing EGFP under the control of the EF1-alpha promoter was derived from the Toledo strain. The gene coding for EGFP was inserted between US9 and US10 of the human CMV genome, a site that appears to tolerate alterations without affecting viral replication. EGFP expression and replication capability were tested on normal human fibroblasts and U-373 human glioblastoma cells [33, 34]. Human dermal fibroblasts were used for viral propagation and titering by plaque assay.

Recombinant CMVs were generously provided by E. Mocarski (Emory University, Atlanta) and J. Vieira (University of Washington, Seattle).

VSV-GFP

A recombinant variant of the Indiana serotype of VSV expressing a GFP reporter gene from the first genomic position (VSV-1'GFP) [35] was kindly provided by J. K. Rose (Yale University, New Haven, CT). Vero cells were used for viral propagation and titering by plaque assay [36].

All the viruses used in the present study express EGFP as a reporter and green fluorescence was employed to visualize infected cells and viral plaques. Viral titers were determined by standard plaque assay using 25% carboxy-methyl-cellulose (CMC) overlay for mCMV-GFP and hCMV-GFP [37] or 0.5% agar overlay for VSV-GFP. Viral stocks were stored in aliquots at −80°C. For each experiment, a new aliquot of virus was thawed and used.

Chemicals

Valpromide (catalog no. V3640), valnoctamide (catalog no. V4765), valproate (catalog no. S0930000), ivermectin (catalog no. I88998), ganciclovir (catalog no. G2536), and heparan sulfate sodium salt (catalog no. H7640) were purchased from Sigma-Aldrich (St. Louis, MO). Valproate and heparan sulfate were dissolved in water to give a stock solution of 1 M and 1 mg/mL, respectively. Valpromide, valnoctamide, ivermectin, and ganciclovir were dissolved in dimethylsulfoxide (DMSO) to yield a stock solution of 1 M (valpromide, valnoctamide) and 100 mM (ivermectin, ganciclovir). Ivermectin was used at 1 μM, a concentration recently shown effective against Chikungunya and other alphaviruses [38].

Quantification of infection

Effects of the tested compounds on CMV infection were assessed by counting the number of infected GFP-positive cells and viral plaques, and measuring plaque size.

Cells (NIH/3T3, Neuro-2a, mouse glia, Vero, normal human dermal fibroblasts, and U-373) were seeded at a density of 40,000 cells per well in 48-well plates and incubated overnight before medium (0.2 mL per well) was replaced for pre-treatment with VPA, VPD, VCD, ivermectin, or vehicle at the specified concentrations. After 24 hours of drug exposure, cells were inoculated with virus and incubated at 37°C for 2 hours. Following incubation, cultures were washed twice with PBS and replenished with fresh media containing the test compounds. GFP-positive cells were counted at 48 (mCMV) and 72 (hCMV) hours post-infection (hpi). In addition, media was collected at 72 (mCMV) or 96 (hCMV) hpi and titered by plaque assay using NIH/3T3 (mCMV) and HDF (hCMV) monolayers to assess the drug-mediated inhibition of virus replication (virus yield reduction assay).

For the plaque reduction assay, cells pre-treated with drugs or vehicle for 24 hours were infected with mCMV-GFP or hCMV-GFP, incubated for 2 hours at 37°C to allow viral adsorption, rinsed twice with PBS, and overlaid with a viscous solution containing the tested agents at the specified concentrations in DMEM (75%) and CMC (25%) for 50% effective concentrations (EC_{50}) calculation [37]. Plates were then incubated at 37°C in 5% CO_2 for 4 days (mCMV) and 7 days (hCMV), to allow time for fluorescent plaques development. The mean plaque counts for each drug concentration were expressed as a percentage of the mean plaque count of the control (vehicle). The EC_{50} were then calculated by nonlinear regression from the plots of log drug concentrations against percentage of reduction in plaque number at each antiviral compound concentration.

To assess which step of the viral replicative cycle was affected by VPD and VCD, ‘time-of-drug addition’ experiments were performed, in which cultures were inoculated with virus (t=0) and exposed to the drugs simultaneously, or 2 hours or 12 hours after viral challenge. The effects of the tested agents on CMV infection were then assessed by a viral yield reduction assay. Briefly, HDF cells were infected with hCMV-GFP (multiplicity of infection, MOI 0.01) (t=0), exposed to the compounds (100 μM) as indicated above, and incubated until the media was collected at 96 hpi. The extent of virus replication was subsequently assessed through titering the media by plaque assay using HDF monolayers. In all conditions, 2 hpi cultures were rinsed twice with PBS to synchronize infection.

Infected cells were identified as GFP-positive cells using an Olympus IX71 fluorescence microscope (Olympus Optical, Tokyo, Japan) connected to a SPOT RT digital camera (Diagnostic Instruments, Sterling Heights, MI) interfaced with an Apple Macintosh computer. The total number of fluorescent cells per well in each condition was counted by two observers independently.

Each condition was tested at least in triplicate, and the whole experiment repeated twice. Camera settings (exposure time and gain) were kept consistent between images. The contrast and color of collected images were optimized using Adobe Photoshop.

To investigate the effects on the immediate early phase of viral replication, NIH/3T3 cells exposed to VPD (1 mM) for 24 hours, were transfected with a CMV promoter (IE1/IE2)-driven reporter plasmid (pCMV-tdTomato) expressing the red fluorescent protein tdTomato.

Virucidal activity assay

To assess the potential virucidal effect of the compounds, VPD, VCD, or vehicle (100 μm) were added to undiluted aliquots of hCMV-GFP and these virus/compound mixtures were incubated at either 4°C or 37°C for 2 hours. After incubation, the samples were diluted with culture medium to reduce the drug concentration to an ineffective dose (10 nM in the antiviral assay), and hCMV-GFP infectivity was determined by plaque assay on HDF cells. Alternatively, virus and drug mixtures were run through a 0.1 μm filter (Life Sciences) to remove the compounds but not the hCMV (size ~180 nm). Filter membranes were subsequently thoroughly rinsed in culture medium for 2 hours at room temperature with periodic shaking to harvest drug-free hCMV before assessing infectivity by plaque assay on HDF monolayers.

Viral entry analysis

To evaluate the effects of the drugs on viral entry into the cell, i.e. reversible attachment of hCMV to the cell membrane and subsequent irreversible binding with fusion and adsorption, inoculated cultures were first incubated at 4°C (which allows only virus attachment) and then shifted to 37°C (which allows fusion and subsequent steps of the viral replication cycle) [3, 39]. Precisely, for assessing the ‘attachment’ step, pre-chilled HDF cells at 90% confluency in a 6-well plate were treated with VPD, VCD, vehicle (100 μM), VPA (1 mM, negative control), or heparan sulfate (0.1 mg/mL, positive control) for 30 minutes at 4°C and inoculated with pre-cooled hCMV-GFP (MOI 0.1) in the presence of compounds or vehicle for 2 hours at 4°C. Fibroblasts were then rinsed three times with cold PBS to remove unattached virions and compounds, and harvested by trypsinization for DNA extraction in the quantitative PCR (qPCR) assay [39] or overlaid with CMC and incubated for 3 days at 37°C for infectivity assessment by GFP-positive cell counting. To evaluate the ‘fusion’ step of the hCMV entry, cultures plated in plain media were inoculated with hCMV-GFP (MOI 0.1) and incubated at 4°C for 2 hours. Cells were then washed three times, exposed to compounds or vehicle at the same concentrations described above, and incubated at 37°C for 2 hours before being overlaid with CMC for infectivity evaluation at 72 hpi.

Quantitative real-time PCR assay

DNA samples were prepared from the hCMV-infected cells in the viral entry experiment using a commercial kit (QIAamp DNA mini kit; Qiagen). Quantitative real time PCR (qPCR) assays for hCMV UL132 (Pa03453400_s1) and human albumin (Hs99999922_s1) genes were performed using TaqMan gene expression assays (Life Technologies) [40, 41]. Ten-fold dilutions of hCMV DNA and cellular DNA from human fibroblasts were used as quantitative standards. qPCR was carried out with 20-μL reaction mixtures employing the iTaq Universal SYBR Probes Supermix (BioRad) and 100 ng of DNA. Samples from uninfected cells and without template served as negative controls. Samples from 2 biological replicates were run in duplicate using a Bio-Rad iCycler-IQ instrument (Bio-Rad, Hercules, CA), and results were analyzed with iCycler software. For the relative quantification of hCMV DNA expression, the comparative threshold cycle (C_T) method was employed and results presented as mean ± SEM of the fold change ($2^{-\Delta\Delta CT}$) relative to the control (vehicle).

Immunocytochemistry

A mouse monoclonal antibody (a gift of Dr. P. Cresswell, Yale University) against hCMV glycoprotein B (gB), diluted 1:1000 in phosphate-buffered saline with 0.3% Triton X-100, was used to label cells infected with hCMV, as an alternative method to the GFP reporter used for quantification of infection. A mouse monoclonal antibody against hCMV immediate early (IE)1/2 antigen (1:1000, MAB810, EMD Millipore) was employed to assess drug-mediated effects on IE proteins expression. The secondary antibody was a goat anti-mouse immunoglobulin conjugated with Alexa Fluor 594 (Thermo Fisher Scientific) diluted at 1:500. Cell nuclei were counterstained with DAPI (4’–6’-diamidino-2-phenylindole). Controls included the omission of the primary antibody and the use of non-inoculated cultures where no immunostaining was expected or found.

Cytotoxicity assay

An ethidium homodimer assay (EthD-1, Molecular Probes, Eugene, OR) was used to label dead cells. Briefly, NIH/3T3 cells (9×10^4 per well) were seeded in a 48-well plate and treated with VPD, VCD, or vehicle for 24 hours before mCMV-GFP inoculation (MOI 0.03). 72 hours after viral challenge, cells were washed twice and EthD-1 was added at a final concentration of 4 μM in DMEM. After 20 minutes of incubation at 37°C, the total number of dead cells per well was counted based on red fluorescence of nuclei. Each condition was tested in quadruplicate, and each experiment was repeated twice. Similarly, the rate of cell death was assessed in uninfected NIH/3T3 and HDF cells exposed to VPD, VCD, vehicle (10 and 1 mM) or plain media for 24 and 72 hours before EthD-1 addition.

Plaque size assay

Plaque size was used to assess the effect of the drugs on viral propagation. Briefly, semiconfluent NIH/3T3 and HDF cells in 12-well plates were inoculated using mCMV-GFP and hCMV-GFP (MOI 1), respectively. After 2 h-incubation at 37°C to allow viral adsorption, inoculum was removed and cultures were washed three times with PBS before the addition of CMC overlay containing VPD, VCD, or vehicle at the specified

concentrations. Five (mCMV) and 10 (hCMV) days later, the relative size of viral plaques was measured (n=60 plaques/condition), as previously described [42]. Each condition was tested at least in triplicate, and the experiment repeated twice. All measurements were performed at the same time using similar camera settings (exposure time and gain).

Animal procedures

Male and female Balb/c strain mice (6–8 weeks of age) from Taconic Biosciences Inc (Hudson, NY) were maintained on a 12:12-h light cycle under constant temperature (22 ± 2 °C) and humidity (55 ± 5 %), with access to food and water *ad libitum*. One to two females were cohabited with a male of the same strain for at least 1 week to ensure fertilization. When advanced pregnancy was seen, each pregnant female was caged singularly and checked for delivery twice daily, at 8:30 AM and 6:30 PM. Newborns were inoculated intraperitoneally (i.p.) with 750 plaque-forming unit (PFU) of mCMV-GFP in 50 μL of media on the day of birth (DOB), within 14 hours of delivery. The DOB was considered postnatal day (PND) 0. Control animals received 50 μL of media i.p.. Infected pups were randomly assigned to receive VPD, VCD, or vehicle (DMSO), via subcutaneous (s.c.) injections, once a day, at a dose of 1.4 mg/mL in 20 μL of saline (~30 μg), starting after virus inoculation from PND 1 to PND 21. Control pups received a similar amount of drug-free saline. Mice were monitored daily for survival until PND 49. Additionally, on each day from PND 0 to 22, without knowledge of the treatment group, pups were weighed to the nearest 0.01 g and their body and tail lengths were measured. Hair growth, status of eyelid and pinnae detachment, and incisor eruption, as compared to adult mice, were also recorded, as previously described [43]. Briefly, these somatic variables were rated semi-quantitatively in the following way: 0 = no occurrence of the condition, 1= slight/uncertain condition, 2 = incomplete condition, and 3 = a complete adult-like condition. For detection of infectious viral load in organs, some of the control and experimental mice were sacrificed on PND 12, after receiving saline/treatment from PND 1 to PND 10. Designated mice were transcardially perfused with PBS, to wash out free virus, and tissue samples were collected under sterile conditions from liver and lungs, two organs markedly involved in severe perinatal infection in humans. Tissues were mechanically homogenized in PBS using a microcentrifuge tube tissue grinder. Part of the resulting tissue suspension was plated onto NIH/3T3 monolayers and viral titer was assessed by plaque assay [37, 44]. All animal breeding and experiments were performed in accordance with the guidelines of the Yale School of Medicine Institutional Animal Care and Use Committee (IACUC). Research was approved by the IACUC.

Statistical analysis

Statistical significance in in vitro experiments was determined using one-way Analysis of Variance (ANOVA), followed by post-hoc analysis (Bonferroni's test). Data are presented as percentage of infected or dead cells, and as viral titers, in drug versus vehicle, as mean ± SEM of two independent experiments; each independent experiment consisted of three or four cultures; p-values refer to a comparison of drug to control (vehicle). Fifty percent effective concentration (EC_{50}) values were calculated using nonlinear regression curve fit with a variable slope (log[inhibitor] vs response). For markers of somatic development, a mixed-model ANOVA with PND as the Repeated Measures factor was used, followed by

Newman Keuls test only if a significant F-value was determined. Analysis was performed with GraphPad Prism 6.0 and SPSS Statistics 21, with significance set at $p \leq 0.05$. Survival studies and assessment of somatic development parameters were performed blindly with respect to the experimental group.

Results

Valpromide inhibits mouse and human CMV in vitro

We performed experiments with several cell types treated with VPA, VPD, or vehicle for 24 hours before viral challenge. VPA (Fig. 1A) increased infection by and replication of mCMV on mouse cells at concentrations of 1 and 10 mM, as previously reported (Fig. 1, B to D) [25–27]. Remarkably, VPD (Fig. 1E) at the same concentrations showed a robust inhibitory effect (Fig. 1, F to H), reducing the number of mCMV-infected cells, as quantified by counting cells expressing the viral GFP reporter gene. VCD also attenuated mCMV replication, assessed by a viral yield assay. Significant inhibition was also identified at lower doses of 100 μM, 1 μM, and 100 nM. Attenuation of mCMV was confirmed at high virus titer and in multiple cell types including NIH/3T3, neuro-2a and primary astrocytes from mouse brain (Fig. 1, I to L). Using an EthD-1 assay to fluorescently label dead cells, VPD at 1 and 10 mM showed no detectable cytotoxicity in uninfected NIH/3T3 cells treated for 24 or 72 hours (Fig. 1M), thus suggesting a lack of toxicity of the target cells even at high drug concentrations and with prolonged cell exposure. In turn, VPD-related CMV inhibition increased cell survival by reducing viral-mediated cytotoxicity (Fig. 1, N and O).

To determine if the inhibitory action of VPD would generalize from mCMV to hCMV, we tested VPD against hCMV on human cells. Similar to mCMV, hCMV infection was enhanced by VPA and substantially inhibited by VPD at 1 and 10 mM, independent of virus titer or cell type (Fig. 2, A to D). VPD significantly reduced the number of hCMV infected cells and also reduced hCMV replication even at the lower drug concentrations of 100 μM, 1 μM, and 100 nM. We found similar inhibitory actions with both human dermal fibroblasts and human glioma cells (U-373). To corroborate the view that the drug acted on CMV rather than by inhibiting expression of the viral GFP reporter, we used immunocytochemistry to label the hCMV glycoprotein B (gB) (Fig. 2E). VPD decreased the number of cells showing hCMV gB immunoreactivity compared to infected cultures not treated with VPD, further corroborating the antiviral effect of VPD on CMV and excluding a potential VPD-mediated inhibitory effect on GFP expression.

Fibroblasts treated with VPD displayed a substantial dose-dependent inhibition of mCMV and hCMV infectivity in the plaque reduction assay with EC_{50} concentrations of 6.8 ± 2.8 μM and 2.9 ± 1.3 μM (Fig. 2F), respectively. The absence of cytotoxic effects at the high dose of 10 mM gives VPD an excellent selectivity index (SI), i.e. the ratio of cytotoxic concentration $(CC)_{50}$ to EC_{50}, for both viruses. An effective antiviral activity was still evident in the nanomolar range, i.e. 100 nM (mCMV: 79% ± 3% infected cells as compared to vehicle-treated controls, p=0.01; hCMV: 77% ± 2%, p=0.004).

The VPD-mediated inhibition of both mouse and human CMV raised the question of whether the antiviral effect of the drug was universal for different types of virus and might

act via enhancement of an innate immune block of virus infection in general. To address this question, we tested VSV, an unrelated single-strand RNA virus sensitive to upregulation of innate immunity. In contrast to mCMV and hCMV, VPD did not inhibit VSV (Fig. 2G), suggesting that VPD antiviral actions were not based on a mechanism involving an enhancement of the innate immune response.

We also tested ivermectin, a compound with anti-epileptic properties and a strong antiparasitic activity which was recently shown to attenuate alphavirus infection [38]. Ivermectin had no effect on CMV (99% ± 9% compared to control), demonstrating that the anti-CMV effect was specific for VPD.

Together these results demonstrate that VPD substantially and selectively inhibits mouse and human CMV infectivity in vitro, and that this antiviral activity is independent of virus titer and cell type.

Valnoctamide, a safer analog of VPD, blocks mouse and human CMV in cell culture

Although VPD safety has been demonstrated in animal models of teratogenesis [10, 11, 17], these findings may not translate to humans where VPD can be quickly metabolized (>80%) to VPA [16], which is both teratogenic and enhances CMV infection as shown earlier. Valnoctamide (VCD) is structurally similar to VPD (Fig. 3A), and lacks the free carboxylic group and HDAC inhibitory activity associated with the embryotoxic and teratogenic effects of VPA [45–47]. However, unlike VPD, VCD shows negligible conversion to its corresponding free acid (valnoctic acid) in humans. VCD was originally marketed as an anxiolytic drug (Nirvanil®) in several European countries in the 1960s and recently investigated as therapeutic agent for seizure disorders and acute mania in humans [45, 46, 48–53]. In contrast to VPA, a number of animal studies have shown no embryotoxicity or teratogenic activity of VCD [10, 47, 49, 54]. Further confirmation of VCD's safety profile is demonstrated from both pre-clinical and clinical studies examining its anti-convulsant and mood stabilizing actions [45, 46, 50–53]. Therefore, we tested VCD on mCMV and hCMV in vitro.

VCD induced a substantial inhibition of mCMV infection independent of cell type or virus titer (Fig. 3, B to F), as measured by counting cells expressing the GFP virus reporter or assessing virus replication. Significant anti-CMV activity was still identified in the nanomolar range. The plaque reduction assay showed a robust dose-dependent inhibition of mCMV infectivity, with an EC_{50} concentration of 9.3 ± 3.5 μM (Fig. 3G). Similar to VPD, VCD at 1 and 10 mM displayed no cytotoxic effect in uninfected NIH/3T3 cells (Fig. 3H), thus defining a SI >1,000 for mCMV.

VCD also blocked infectivity and replication of hCMV at low and high titer in human fibroblasts (Fig. 3, I to L), and dose-response analysis revealed an EC_{50} of 3.5 ± 1.1 μM (Fig. 3M). Again, no cytotoxicity was evident in uninfected human fibroblasts exposed to 1 and 10 mM VCD, thus conferring the drug a SI >2,800 for hCMV.

Dose-response analysis of known antiviral compounds by plaque reduction assay

The antiviral properties of well-known inhibitors of CMV infection, ganciclovir (GCV) and heparan sulfate (HS), were assessed for comparative purposes in a dose-escalation analysis by plaque reduction assay in HDF cells infected with hCMV (MOI 0.01), as performed for VPD and VCD.

GCV targets viral DNA polymerase and is approved for CMV treatment in humans [5]. HS acts as a soluble mimic of heparan sulfate proteoglycans (HSPGs), cell surface anionic polysaccharides used by CMV for attachment to the cell [55]. HS is not an approved anti-CMV drug due to its strong anticoagulant activity in vivo, an undesired side-effect.

Human CMV infectivity was inhibited by both GCV and HS in a dose-dependent manner with EC_{50} of 1.1 ± 0.3 μM for GCV (Fig. 3N) and 51.4 ± 8.2 μg/mL (~80 μM) for HS (Fig. 3O).

Valpromide and valnoctamide substantially attenuate CMV-related disease in vivo

Perinatal hCMV infection can cause serious and potentially fatal disease in neonates [3], in whom therapeutic options are severely limited by the toxicity and carcinogenicity of available antiviral drugs [5].

Prior to testing anti-CMV efficacy, we evaluated drug safety with daily administration of both compounds in control, uninfected developing mice. No adverse effects on survival (data not shown) or post-natal body growth (Fig. 4A) were detected.

Inasmuch as the drugs appeared safe in developing mice, we next assessed VPD and VCD in a mouse model of severe perinatal mCMV infection (Fig. 4B) [56]. VPD and VCD treatment induced substantial improvement in infected newborns health, with a three-fold decrease in death rate (Fig. 4C). Survival of mCMV-infected, untreated pups was 23%, compared to 72% for VPD-or VCD-treated mice. Additional benefits of drug treatment were also identified. VPD and VCD administration ameliorated the mCMV-induced detrimental effects on body growth as assessed by body weight, body length, and tail length (Fig. 4, D to G); infected mice weighed nearly 50% less than control mice at postnatal day 20 ($p < 0.001$), whereas VPD- or VCD-treated infected pups showed a body weight reduction of only 18% (Fig. 4E). Thus, both VPD and VCD attenuated the deficient body growth induced by perinatal mCMV infection. Both drugs markedly improved other parameters of somatic development, including eyelid opening, pinnae detachment, fur maturation, and incisor eruption (Fig. 5, A to F). Of note, VPD and VCD generated a significant ($p<0.01$) improvement in CMV-infected neonate health as early as 5 days after initiation of treatment.

After intraperitoneal inoculation, CMV infection spreads to several organs, including liver, spleen, and lungs. To investigate whether the beneficial effects observed in the infected pups were related to the ability of VPD and VCD to decrease CMV levels, we analyzed these organs from infected mice at 12 dpi by viral plaque assay (Fig. 6, A to D). CMV titers were decreased by greater than 2 logs in all tested tissues of drug-treated infected newborns, thus suggesting that the VPD- and VCD-mediated inhibitory effects on CMV infection observed

in vitro also occur in vivo and lead to a substantial improvement in CMV-infected animal outcome.

Valpromide and valnoctamide suppress CMV by inhibiting virus attachment to the cell

Despite being used for decades to treat neurological dysfunctions, the mechanism(s) of action of VPD and VCD in the brain remain unclear [8, 46, 57]. VPA-mediated inhibition of HDAC enhances infection by hCMV [25–27]. Both VPD and VCD lack this epigenetic activity [11, 17].

To gain insight into the underlying mechanisms of VPD and VCD inhibition of CMV, we tested the drugs by addition at different time-points during the course of hCMV infection (Fig. 7A). The drug concentration employed for testing was 100 μM, which is below the therapeutic range for safely treating mood disorders and epilepsy in humans [28–30, 46, 47, 52, 53, 57–59]. When the compounds were present from the time of viral challenge through 96 hpi, viral yield decreased 60%. A similar inhibition of hCMV replication was also observed with 2 hr drug exposure at the time of viral challenge, followed by drug wash out (data not shown). However, no reduction in viral yield was identified when the compounds were added 2 to 12 hours after virus inoculation (Fig. 7A).

These results indicate that the block of hCMV mediated by VPD and VCD is exerted early in the infection process, within the first 2 hours of the replication cycle. We therefore tested the possibility that these agents directly inactivate virions by pre-incubating the compounds with an undiluted stock of hCMV prior to cell inoculation. When the inhibitors were subsequently diluted below an effective concentration prior to culture inoculation, no direct inactivation of free virions was observed, as determined by the absence of a drug-mediated inhibitory effect (Fig. 7B). Similar results were obtained when the pre-incubation mix was run through a 100 nm pore size filter to remove the compounds but not the virus, prior to analysis of virus infectivity at physiological and cold temperatures (percentages show hCMV viral titers in drug-treated samples as compared to vehicle: 37°C, 98.5 ± 8% for VPD, 99.3% ± 5% for VCD; 4°C, 100.6% ± 5% for VPD, 98.3% ± 8% for VCD).

The IE1/2 CMV promoter is active in the first few hours of CMV infection, inducing IE protein expression which in turn promotes viral replication [3]; we investigated whether the drugs interfere with activity of this promoter by testing a plasmid with CMV IE1/2 driving tdTomato expression. No decrease in the number of red cells was identified in the presence of VPD compared to control (96% ± 4%) after plasmid transfection, suggesting VPD does not inhibit the activity of the CMV IE1/2 promoter. In addition, we assessed IE1/2 antigen expression in hCMV infected cells exposed to the compounds either simultaneously or 2 hours after viral challenge (Fig. 7C). Substantial IE1/2 was detected in fibroblasts that received vehicle or drugs after 2 hpi. In contrast, cells treated with the compounds at the time of CMV inoculation showed markedly decreased IE1/2 expression, thus suggesting that CMV inhibition by VPD and VCD occurs prior to the IE stages of the viral replication cycle.

We next examined CMV entry into the cell, which precedes IE protein expression and can be separated into two phases: (1) attachment of the viral particle to the cell surface and (2) fusion of the viral envelope with cellular membranes and penetration into the cytoplasmic

space [3]. Investigation of these phases by a 2 hr incubation at 4°C (a temperature that allows attachment but not fusion) followed by a temperature shift to 37°C (which allow fusion) [39] and subsequent infectivity assessment by GFP-positive cells counting, showed VPD- and VCD-mediated interference with hCMV attachment to the cell (Fig. 7D). These results were confirmed by qPCR with quantification of the relative amount of hCMV DNA in infected human fibroblasts exposed to the compounds at 4°C (Fig. 7E). In these assays, heparan sulfate was employed as positive control given its ability to block CMV attachment in vitro by mimicking HSPGs [55].

Current approved anti-CMV compounds target viral DNA synthesis (GCV, foscarnet, cidofovir) or the hCMV major IE gene locus (fomivirsen). Since our data indicate that VPD and VCD may block a different, earlier step of CMV infection, similar to HS, we postulated that a combined administration of GCV with VCD or HS might induce a stronger viral inhibition than single drug therapy or VCD/HS association (Fig. 7F). When cells were exposed to both GCV + VCD or GCV + HS, the decrease in hCMV plaques nearly doubled compared to single drug treatment. In contrast, combination of VCD + HS only slightly increased the viral inhibition obtained with one compound, supporting the hypothesis that VPD, VCD, and HS may act on the same step of CMV infection.

Finally, prolonged cell exposure to VPD and VCD followed by drug wash out immediately before CMV inoculation resulted in no attenuation of infection (Fig. 7G), consistent with the view that the drugs did not exert persistent effects on antiviral cellular targets, such as enhancement of innate immunity. These data also suggest that the anti-CMV actions of VPD and VCD are not the result of an irreversible association of the compounds with cell surface proteins.

Valpromide and valnoctamide decrease spread of CMV infection

Inhibition of CMV attachment to the target cell may play a role not only in the initiation of infection but also on virus spread. Murine and human fibroblast cells were exposed to the drugs after CMV inoculation and adsorption, and assessed for viral plaque size at 5 (mCMV) and 10 (hCMV) dpi. Both VPD and VCD effectively decreased spread of the CMV infection as shown by the reduced plaque size in CMV-infected treated monolayers compared with the plaque size from vehicle-treated cultures (Fig. 8, A to C).

Discussion

Human CMV is an important pathogen responsible for potentially life-threatening disease and severe complications, including pneumonitis, retinitis, encephalitis, and myocarditis in immunocompromised patients and neonatal children. Congenital CMV is the major infectious cause of birth defects and neuro-developmental disabilities, such as microcephaly, hearing loss, blindness, and mental retardation [1, 3–5].

Current anti-CMV compounds are partially effective, but are limited by poor oral bioavailability, short- and long-term toxicity, carcinogenicity, and teratogenicity [5]. The emergence of CMV strains resistant to the available drugs also poses significant challenges. Thus, there is a need for novel anti-CMV molecules with a safe in vivo profile utilizing

alternative mechanisms of action. This is particularly relevant to CMV infections during early development.

Our work shows that VPD and VCD, two orally available drugs used for many years to treat neurological disorders, evoke an unexpected, substantial, and specific inhibition of both mouse and human CMV in vitro and in a mouse model of perinatal infection. The anti-CMV activity of these compounds has never been described.

The VPD- and VCD-mediated antiviral effect is substantiated by multiple converging lines of evidence including reduction in infected cell number, as determined with GFP reporter expression, immunocytochemistry against hCMV gB, and qPCR, reduction in cell death quantified with ethidium homodimer, reduction in virus plaque number and size, and reduction in viral replication and virion release. Importantly, both compounds showed efficacy in blocking CMV infection in vivo, leading to increased survival, improved body weight, reduced CMV-related disease, and decreased viral load in target organs of infected neonates. Furthermore, drug administration to uninfected newborn mice evoked no adverse response.

We detected relatively little cell death evoked even at the highest concentrations of VPD and VCD as tested with the ethidium homodimer assay; we did not study the effects of the drugs on cell metabolism. VPD and VCD inhibited CMV at drug concentrations already safely employed in the clinic for anti-convulsant and mood stabilizing purposes (roughly 0.2 to 0.7 mM), and, more importantly, at lower drug concentrations (≤ 100 μM) which lack neurological and psychiatric effects in humans [28–30, 46, 47, 52, 53, 57–59]. Thus, a safe and effective anti-CMV activity of these compounds in humans seems plausible.

Currently approved anti-CMV drugs generally target hCMV IE gene expression or DNA replication [5]. In contrast, VPD and VCD appear to act on an earlier stage of CMV infection by interfering with viral attachment to cell surface HSPGs. The initial tethering of CMV virions to HSPGs, mediated by the viral glycoproteins gB and gM/gN, functions to stabilize the virus at the cell surface until engagement of secondary receptors occurs allowing fusion and penetration [3, 60]. The VPD and VCD drug-mediated inhibition of hCMV attachment may be due to a reversible interaction with either HSPGs or free virions or may require the simultaneous presence of both the virus and the cell.

Dose-response relationship analyses revealed that GCV, currently a first-line therapy for hCMV, is a more potent compound than VPD and VCD in vitro. Thus, a less effective anti-CMV activity of VPD and VCD compared to GCV might be expected in vivo. However, given the increasing emergence of drug-resistant strains of hCMV and the potential toxicity related to long-term therapy with GCV, compounds with an alternative mechanism of action merit consideration for anti-CMV clinical trials. We show that VPD and VCD used together with GCV generate an additive effect in blocking CMV; the combination of the two drug types acting by different mechanisms of inhibition may also constitute a fertile ground for clinical consideration.

Conclusions

We examined two drugs, VPD and VCD, which show unexpected anti-CMV properties. In humans, VPD can be metabolized to the teratogenic and CMV-enhancing VPA [16], and therefore would not be an ideal drug candidate in the clinic, particularly in the treatment of pregnant mothers and their fetuses. VCD lacks embryotoxic and teratogenic actions [45–47], and in contrast to VPD shows minimal conversion to its corresponding free acid in humans [45]. Therefore, VCD may merit consideration as a potential mode of treatment to reduce the severity of problems caused by CMV infection in conditions of reduced systemic immunity. Furthermore, there is a need for anti-CMV drugs that are safe and effective in the treatment of CMV in fetuses and neonates, and VCD merits further consideration in this regard. The fact that VCD is already approved for the treatment of neurological and psychiatric disorders in humans should greatly reduce the typically long period required to bring a new antiviral drug into use.

Acknowledgments

We thank Yang Yang for technical help, Zhonghua Tang and Seth Guller for help with the qPCR experiment, and Justin Paglino for comments on the manuscript. This work was supported by funds from Amalia Griffini Scholarship (S.O.), rEVO Biologics (M.J.P.), and National Institutes of Health RO1 CA188359, CA175577, CA161048, and NS79274 (A.v.d.P). Funding sources had no involvement in study design; collection, analysis and interpretation of data; writing of the report; and decision to submit the article for publication.

References

1. Cheeran MC, Lokensgard JR, Schleiss MR. Neuropathogenesis of congenital cytomegalovirus infection: disease mechanisms and prospects for intervention. Clinical microbiology reviews. 2009; 22(1):99–126. Table of Contents. Epub 2009/01/13. PubMed PMID: 19136436; PubMed Central PMCID: PMCPMC2620634. [PubMed: 19136436]
2. Gandhi MK, Khanna R. Human cytomegalovirus: clinical aspects, immune regulation, and emerging treatments. The Lancet Infectious diseases. 2004; 4(12):725–738. Epub 2004/11/30. PubMed PMID: 15567122. [PubMed: 15567122]
3. Mocarski, ES.; Shenk, T.; Pass, RF. Cytomegaloviruses. In: Fields, BN.; Knipe, DM.; Howley, PM., editors. Fields Virology. Vol. 2. Philadelphia, PA: Lippincott, Williams & Wilkins; 2007. p. 2702-2751.
4. Tsutsui Y. Effects of cytomegalovirus infection on embryogenesis and brain development. Congenital anomalies. 2009; 49(2):47–55. Epub 2009/06/06. PubMed PMID: 19489954. [PubMed: 19489954]
5. Mercorelli B, Lembo D, Palu G, Loregian A. Early inhibitors of human cytomegalovirus: state-of-art and therapeutic perspectives. Pharmacology & therapeutics. 2011; 131(3):309–329. Epub 2011/05/17. PubMed PMID: 21570424. [PubMed: 21570424]
6. Perucca E. Pharmacological and therapeutic properties of valproate: a summary after 35 years of clinical experience. CNS drugs. 2002; 16(10):695–714. Epub 2002/09/25. PubMed PMID: 12269862. [PubMed: 12269862]
7. Guerrini R. Valproate as a mainstay of therapy for pediatric epilepsy. Paediatric drugs. 2006; 8(2): 113–129. Epub 2006/04/13. PubMed PMID: 16608372. [PubMed: 16608372]
8. Monti B, Polazzi E, Contestabile A. Biochemical, molecular and epigenetic mechanisms of valproic acid neuroprotection. Current molecular pharmacology. 2009; 2(1):95–109. Epub 2009/12/22. PubMed PMID: 20021450. [PubMed: 20021450]
9. Nau H, Hauck RS, Ehlers K. Valproic acid-induced neural tube defects in mouse and human: aspects of chirality, alternative drug development, pharmacokinetics and possible mechanisms.

Pharmacology & toxicology. 1991; 69(5):310–321. Epub 1991/11/01. PubMed PMID: 1803343. [PubMed: 1803343]

10. Radatz M, Ehlers K, Yagen B, Bialer M, Nau H. Valnoctamide, valpromide and valnoctic acid are much less teratogenic in mice than valproic acid. Epilepsy research. 1998; 30(1):41–48. Epub 1998/04/29. PubMed PMID: 9551843. [PubMed: 9551843]
11. Okada A, Kurihara H, Aoki Y, Bialer M, Fujiwara M. Amidic modification of valproic acid reduces skeletal teratogenicity in mice. Birth defects research Part B, Developmental and reproductive toxicology. 2004; 71(1):47–53. Epub 2004/03/03. PubMed PMID: 14991910.
12. Phiel CJ, Zhang F, Huang EY, Guenther MG, Lazar MA, Klein PS. Histone deacetylase is a direct target of valproic acid, a potent anticonvulsant, mood stabilizer, and teratogen. The Journal of biological chemistry. 2001; 276(39):36734–36741. Epub 2001/07/27. PubMed PMID: 11473107. [PubMed: 11473107]
13. Tung EW, Winn LM. Epigenetic modifications in valproic acid-induced teratogenesis. Toxicology and applied pharmacology. 2010; 248(3):201–209. Epub 2010/08/14. PubMed PMID: 20705080. [PubMed: 20705080]
14. Paradis FH, Hales BF. Exposure to valproic acid inhibits chondrogenesis and osteogenesis in mid-organogenesis mouse limbs. Toxicological sciences : an official journal of the Society of Toxicology. 2013; 131(1):234–241. Epub 2012/10/09. PubMed PMID: 23042728; PubMed Central PMCID: PMCPMC3537135. [PubMed: 23042728]
15. Kataoka S, Takuma K, Hara Y, Maeda Y, Ago Y, Matsuda T. Autism-like behaviours with transient histone hyperacetylation in mice treated prenatally with valproic acid. The international journal of neuropsychopharmacology / official scientific journal of the Collegium Internationale Neuropsychopharmacologicum (CINP). 2013; 16(1):91–103. Epub 2011/11/19. PubMed PMID: 22093185.
16. Bialer M. Clinical pharmacology of valpromide. Clinical pharmacokinetics. 1991; 20(2):114–122. Epub 1991/02/01. PubMed PMID: 2029804. [PubMed: 2029804]
17. Fujiki R, Sato A, Fujitani M, Yamashita T. A proapoptotic effect of valproic acid on progenitors of embryonic stem cell-derived glutamatergic neurons. Cell death & disease. 2013; 4:e677. Epub 2013/06/22. PubMed PMID: 23788034; PubMed Central PMCID: PMCPMC3702299. [PubMed: 23788034]
18. Gorres KL, Daigle D, Mohanram S, McInerney GE, Lyons DE, Miller G. Valpromide Inhibits Lytic Cycle Reactivation of Epstein-Barr Virus. mBio. 2016; 7(2) Epub 2016/03/05. PubMed PMID: 26933051; PubMed Central PMCID: PMCPMC4810481.
19. Moog C, Kuntz-Simon G, Caussin-Schwemling C, Obert G. Sodium valproate, an anticonvulsant drug, stimulates human immunodeficiency virus type 1 replication independently of glutathione levels. The Journal of general virology. 1996; 77(Pt 9):1993–1999. Epub 1996/09/01. PubMed PMID: 8810995. [PubMed: 8810995]
20. Paglino JC, van den Pol AN. Vesicular stomatitis virus has extensive oncolytic activity against human sarcomas: rare resistance is overcome by blocking interferon pathways. Journal of virology. 2011; 85(18):9346–9358. Epub 2011/07/08. PubMed PMID: 21734048; PubMed Central PMCID: PMCPMC3165768. [PubMed: 21734048]
21. Shaw RN, Arbiser JL, Offermann MK. Valproic acid induces human herpesvirus 8 lytic gene expression in BCBL-1 cells. AIDS (London, England). 2000; 14(7):899–902. Epub 2000/06/06. PubMed PMID: 10839602.
22. Nakashima H, Kaufmann JK, Wang PY, Nguyen T, Speranza MC, Kasai K, et al. Histone deacetylase 6 inhibition enhances oncolytic viral replication in glioma. The Journal of clinical investigation. 2015; 125(11):4269–4280. Epub 2015/11/03. PubMed PMID: 26524593; PubMed Central PMCID: PMCPMC4639993. [PubMed: 26524593]
23. Otsuki A, Patel A, Kasai K, Suzuki M, Kurozumi K, Chiocca EA, et al. Histone deacetylase inhibitors augment antitumor efficacy of herpes-based oncolytic viruses. Molecular therapy : the journal of the American Society of Gene Therapy. 2008; 16(9):1546–1555. Epub 2008/07/24. PubMed PMID: 18648350. [PubMed: 18648350]
24. Mardivirin L, Descamps V, Lacroix A, Delebassee S, Ranger-Rogez S. Early effects of drugs responsible for DRESS on HHV-6 replication in vitro. Journal of clinical virology : the official

publication of the Pan American Society for Clinical Virology. 2009; 46(3):300–302. Epub 2009/09/18. PubMed PMID: 19758840. [PubMed: 19758840]

25. Kuntz-Simon G, Obert G. Sodium valproate, an anticonvulsant drug, stimulates human cytomegalovirus replication. The Journal of general virology. 1995; 76(Pt 6):1409–1415. Epub 1995/06/01. PubMed PMID: 7782769. [PubMed: 7782769]
26. Michaelis M, Kohler N, Reinisch A, Eikel D, Gravemann U, Doerr HW, et al. Increased human cytomegalovirus replication in fibroblasts after treatment with therapeutical plasma concentrations of valproic acid. Biochemical pharmacology. 2004; 68(3):531–538. Epub 2004/07/10. PubMed PMID: 15242819. [PubMed: 15242819]
27. Michaelis M, Suhan T, Reinisch A, Reisenauer A, Fleckenstein C, Eikel D, et al. Increased replication of human cytomegalovirus in retinal pigment epithelial cells by valproic acid depends on histone deacetylase inhibition. Investigative ophthalmology & visual science. 2005; 46(9): 3451–3457. Epub 2005/08/27. PubMed PMID: 16123451. [PubMed: 16123451]
28. Brodie MJ, Dichter MA. Antiepileptic drugs. N Engl J Med. 1996; 334(3):168–175. Epub 1996/01/18. PubMed PMID: 8531974. [PubMed: 8531974]
29. Pisani F, Fazio A, Oteri G, Ruello C, Gitto C, Russo F, et al. Sodium valproate and valpromide: differential interactions with carbamazepine in epileptic patients. Epilepsia. 1986; 27(5):548–552. Epub 1986/09/01. PubMed PMID: 3093212. [PubMed: 3093212]
30. Matalon S, Rasmussen TA, Dinarello CA. Histone deacetylase inhibitors for purging HIV-1 from the latent reservoir. Molecular medicine (Cambridge, Mass). 2011; 17(5–6):466–472. Epub 2011/03/23. PubMed PMID: 21424110; PubMed Central PMCID: PMCPMC3105138.
31. Jennings HR, Romanelli F. Comment: potential risk of valproic acid therapy in patients who are HIV-positive. The Annals of pharmacotherapy. 2000; 34(11):1348–1349. Epub 2000/12/01. PubMed PMID: 11098354. [PubMed: 11098354]
32. van Den Pol AN, Mocarski E, Saederup N, Vieira J, Meier TJ. Cytomegalovirus cell tropism, replication, and gene transfer in brain. The Journal of neuroscience : the official journal of the Society for Neuroscience. 1999; 19(24):10948–10965. Epub 1999/12/14. PubMed PMID: 10594076. [PubMed: 10594076]
33. Vieira J, Schall TJ, Corey L, Geballe AP. Functional analysis of the human cytomegalovirus US28 gene by insertion mutagenesis with the green fluorescent protein gene. Journal of virology. 1998; 72(10):8158–8165. Epub 1998/09/12. PubMed PMID: 9733857; PubMed Central PMCID: PMCPMC110158. [PubMed: 9733857]
34. Jarvis MA, Wang CE, Meyers HL, Smith PP, Corless CL, Henderson GJ, et al. Human cytomegalovirus infection of caco-2 cells occurs at the basolateral membrane and is differentiation state dependent. Journal of virology. 1999; 73(6):4552–4560. Epub 1999/05/11. PubMed PMID: 10233913; PubMed Central PMCID: PMCPMC112495. [PubMed: 10233913]
35. Ramsburg E, Publicover J, Buonocore L, Poholek A, Robek M, Palin A, et al. A vesicular stomatitis virus recombinant expressing granulocyte-macrophage colony-stimulating factor induces enhanced T-cell responses and is highly attenuated for replication in animals. Journal of virology. 2005; 79(24):15043–15053. Epub 2005/11/25. PubMed PMID: 16306575; PubMed Central PMCID: PMCPMC1316007. [PubMed: 16306575]
36. van den Pol AN, Dalton KP, Rose JK. Relative neurotropism of a recombinant rhabdovirus expressing a green fluorescent envelope glycoprotein. Journal of virology. 2002; 76(3):1309–1327. Epub 2002/01/05. PubMed PMID: 11773406; PubMed Central PMCID: PMCPMC135838. [PubMed: 11773406]
37. Zurbach KA, Moghbeli T, Snyder CM. Resolving the titer of murine cytomegalovirus by plaque assay using the M2-10B4 cell line and a low viscosity overlay. Virology journal. 2014; 11:71. Epub 2014/04/20. PubMed PMID: 24742045; PubMed Central PMCID: PMCPMC4006460. [PubMed: 24742045]
38. Varghese FS, Kaukinen P, Glasker S, Bespalov M, Hanski L, Wennerberg K, et al. Discovery of berberine, abamectin and ivermectin as antivirals against chikungunya and other alphaviruses. Antiviral research. 2016; 126:117–124. Epub 2016/01/12. PubMed PMID: 26752081. [PubMed: 26752081]

39. Chan GC, Yurochko AD. Analysis of cytomegalovirus binding/entry-mediated events. Methods in molecular biology (Clifton, NJ). 2014; 1119:113–121. Epub 2014/03/19. PubMed PMID: 24639221.
40. Gault E, Michel Y, Dehee A, Belabani C, Nicolas JC, Garbarg-Chenon A. Quantification of human cytomegalovirus DNA by real-time PCR. Journal of clinical microbiology. 2001; 39(2):772–775. Epub 2001/02/07. PubMed PMID: 11158149; PubMed Central PMCID: PMCPMC87818. [PubMed: 11158149]
41. Fukui Y, Shindoh K, Yamamoto Y, Koyano S, Kosugi I, Yamaguchi T, et al. Establishment of a cell-based assay for screening of compounds inhibiting very early events in the cytomegalovirus replication cycle and characterization of a compound identified using the assay. Antimicrobial agents and chemotherapy. 2008; 52(7):2420–2407. Epub 2008/05/07. PubMed PMID: 18458124; PubMed Central PMCID: PMCPMC2443885. [PubMed: 18458124]
42. Wollmann G, Drokhlyansky E, Davis JN, Cepko C, van den Pol AN. Lassa-vesicular stomatitis chimeric virus safely destroys brain tumors. Journal of virology. 2015; 89(13):6711–6724. Epub 2015/04/17. PubMed PMID: 25878115; PubMed Central PMCID: PMCPMC4468483. [PubMed: 25878115]
43. Scattoni ML, Gandhy SU, Ricceri L, Crawley JN. Unusual repertoire of vocalizations in the BTBR T+tf/J mouse model of autism. PloS one. 2008; 3(8):e3067. Epub 2008/08/30. PubMed PMID: 18728777; PubMed Central PMCID: PMCPMC2516927. [PubMed: 18728777]
44. Brune W, Hengel H, Koszinowski UH. Coligan, John E., et al.A mouse model for cytomegalovirus infection. Current protocols in immunology. 2001; Chapter 19(Unit 19.7) Epub 2008/04/25. PubMed PMID: 18432758.
45. Bialer M, Haj-Yehia A, Barzaghi N, Pisani F, Perucca E. Pharmacokinetics of a valpromide isomer, valnoctamide, in healthy subjects. European journal of clinical pharmacology. 1990; 38(3):289–291. Epub 1990/01/01. PubMed PMID: 2111246. [PubMed: 2111246]
46. Bialer M, Johannessen SI, Levy RH, Perucca E, Tomson T, White HS. Progress report on new antiepileptic drugs: A summary of the Twelfth Eilat Conference (EILAT XII). Epilepsy research. 2015; 111:85–141. Epub 2015/03/15. PubMed PMID: 25769377. [PubMed: 25769377]
47. Shekh-Ahmad T, Hen N, Yagen B, McDonough JH, Finnell RH, Wlodarczyk BJ, et al. Stereoselective anticonvulsant and pharmacokinetic analysis of valnoctamide, a CNS-active derivative of valproic acid with low teratogenic potential. Epilepsia. 2014; 55(2):353–361. Epub 2013/12/10. PubMed PMID: 24313671. [PubMed: 24313671]
48. Stepansky W. A clinical study in the use of valmethamide, an anxiety-reducing drug. Current therapeutic research, clinical and experimental. 1960; 2:144–147. Epub 1960/05/01. PubMed PMID: 13834349.
49. Mawasi H, Shekh-Ahmad T, Finnell RH, Wlodarczyk BJ, Bialer M. Pharmacodynamic and pharmacokinetic analysis of CNS-active constitutional isomers of valnoctamide and sec-butylpropylacetamide--Amide derivatives of valproic acid. Epilepsy & behavior : E&B. 2015; 46:72–78. Epub 2015/04/13. PubMed PMID: 25863940.
50. Winkler I, Blotnik S, Shimshoni J, Yagen B, Devor M, Bialer M. Efficacy of antiepileptic isomers of valproic acid and valpromide in a rat model of neuropathic pain. British journal of pharmacology. 2005; 146(2):198–208. Epub 2005/07/06. PubMed PMID: 15997234; PubMed Central PMCID: PMCPMC1576263. [PubMed: 15997234]
51. Shekh-Ahmad T, Mawasi H, McDonough JH, Yagen B, Bialer M. The potential of sec-butylpropylacetamide (SPD) and valnoctamide and their individual stereoisomers in status epilepticus. Epilepsy & behavior : E&B. 2015; 49:298–302. Epub 2015/05/17. PubMed PMID: 25979572.
52. Barel S, Yagen B, Schurig V, Soback S, Pisani F, Perucca E, et al. Stereoselective pharmacokinetic analysis of valnoctamide in healthy subjects and in patients with epilepsy. Clinical pharmacology and therapeutics. 1997; 61(4):442–449. Epub 1997/04/01. PubMed PMID: 9129561. [PubMed: 9129561]
53. Bersudsky Y, Applebaum J, Gaiduk Y, Sharony L, Mishory A, Podberezsky A, et al. Valnoctamide as a valproate substitute with low teratogenic potential in mania: a double-blind, controlled, add-on clinical trial. Bipolar disorders. 2010; 12(4):376–382. Epub 2010/07/20. PubMed PMID: 20636634. [PubMed: 20636634]

54. Wlodarczyk BJ, Ogle K, Lin LY, Bialer M, Finnell RH. Comparative teratogenicity analysis of valnoctamide, risperidone, and olanzapine in mice. Bipolar disorders. 2015; 17(6):615–625. Epub 2015/08/21. PubMed PMID: 26292082; PubMed Central PMCID: PMCPMC4631615. [PubMed: 26292082]

55. Compton T, Nowlin DM, Cooper NR. Initiation of human cytomegalovirus infection requires initial interaction with cell surface heparan sulfate. Virology. 1993; 193(2):834–841. Epub 1993/04/01. PubMed PMID: 8384757. [PubMed: 8384757]

56. Slavuljica I, Kvestak D, Huszthy PC, Kosmac K, Britt WJ, Jonjic S. Immunobiology of congenital cytomegalovirus infection of the central nervous system-the murine cytomegalovirus model. Cellular & molecular immunology. 2015; 12(2):180–191. Epub 2014/07/22. PubMed PMID: 25042632; PubMed Central PMCID: PMCPMC4654296. [PubMed: 25042632]

57. Spampanato J, Dudek FE. Valnoctamide enhances phasic inhibition: a potential target mechanism for the treatment of benzodiazepine-refractory status epilepticus. Epilepsia. 2014; 55(9):e94–e98. Epub 2014/07/06. PubMed PMID: 24995528; PubMed Central PMCID: PMCPMC4167227. [PubMed: 24995528]

58. Witvrouw M, Schmit JC, Van Remoortel B, Daelemans D, Este JA, Vandamme AM, et al. Cell type-dependent effect of sodium valproate on human immunodeficiency virus type 1 replication in vitro. AIDS research and human retroviruses. 1997; 13(2):187–192. Epub 1997/01/20. PubMed PMID: 9007204. [PubMed: 9007204]

59. Pisani F, Fazio A, Oteri G, Di Perri R. Dipropylacetic acid plasma levels; diurnal fluctuations during chronic treatment with dipropylacetamide. Therapeutic drug monitoring. 1981; 3(3):297–301. Epub 1981/01/01. PubMed PMID: 6798719. [PubMed: 6798719]

60. Isaacson MK, Compton T. Human cytomegalovirus glycoprotein B is required for virus entry and cell-to-cell spread but not for virion attachment, assembly, or egress. Journal of virology. 2009; 83(8):3891–903. Epub 2009/02/06. PubMed PMID: 19193805; PubMed Central PMCID: PMCPMC2663263. [PubMed: 19193805]

Highlights

- Valpromide and valnoctamide are mood stabilizers approved for the treatment of multiple neurological disorders.
- Valpromide and valnoctamide effectively inhibit human and murine cytomegalovirus (CMV) in vitro.
- In a mouse model of perinatal infection, both drugs safely attenuate murine CMV and improve survival and development.
- Valpromide and valnoctamide appear to act by a novel mechanism arising from inhibition of CMV attachment to the cell.

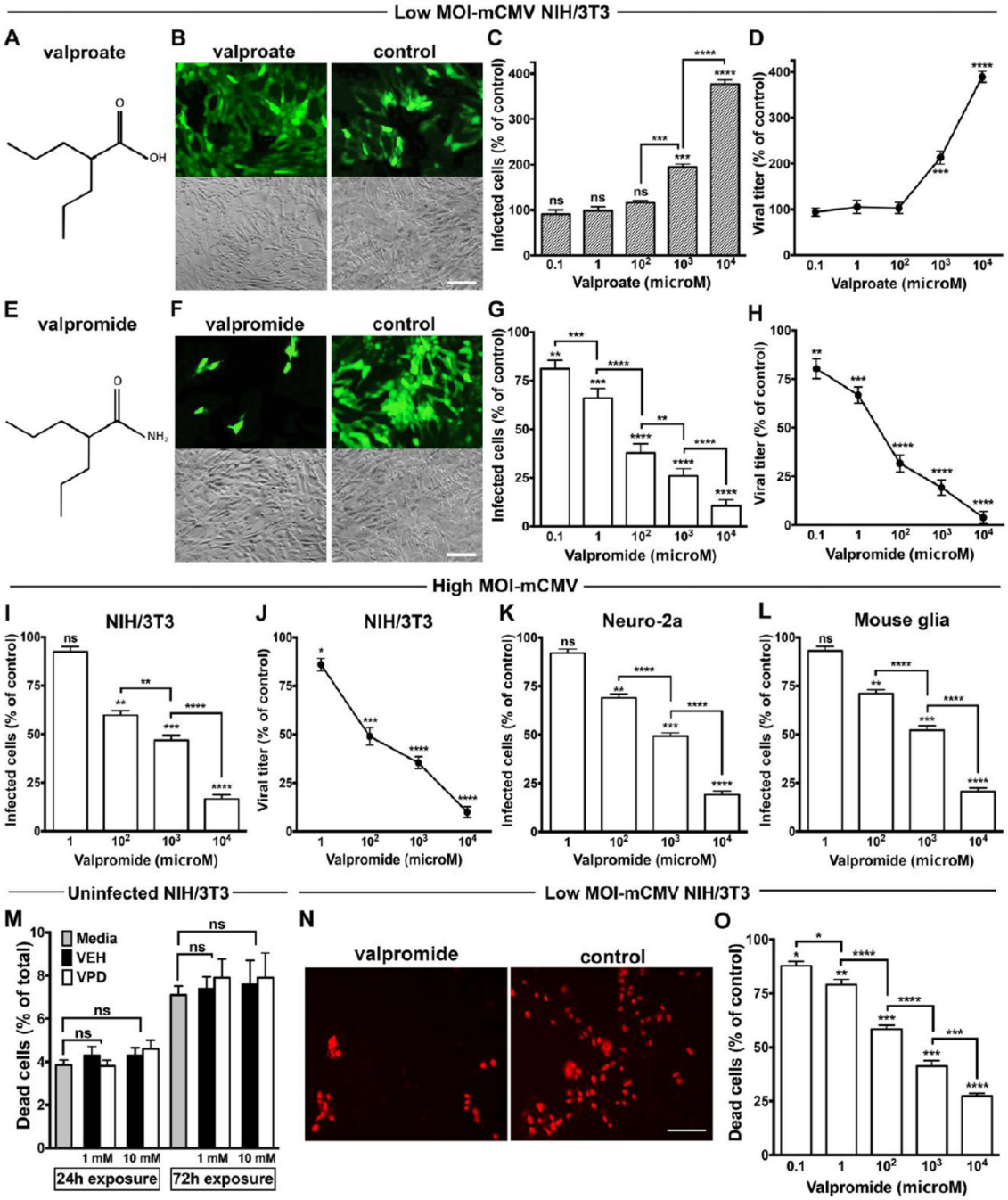

Fig. 1. Valproate and valpromide exert opposing effects on mouse CMV

(**A**) Chemical structure of valproate. (**B**) Representative microscopic fields show mCMV-GFP reporter fluorescence (top) and phase contrast (bottom) of NIH/3T3 cells pre-treated (24hrs) with VPA (1mM) or vehicle prior to inoculation with mCMV using multiplicity of infection (MOI) of 0.03. Photos captured 48 hpi; scale bar 50 μm. (**C** and **D**) VPA dose-dependent increase in mCMV infection assessed by counting infected GFP-positive cells at 48 hpi (C) and viral yield assay at 72 hpi (D); other conditions same as B. (**E**) Chemical structure of valpromide. (**F**) VPD (1mM) with other conditions same as B. (**G** and **H**) VPD

dose-dependent decrease in mCMV infection, as per number of infected cells at 48 hpi (G) and viral titer at 72 hpi (H); other conditions same as B. (**I** to **L**) VPD dose-dependent decrease in mCMV-infectivity in NIH/3T3 (I and J), immortalized Neuro-2a (K) and primary mouse glia (L) cells (MOI 4). Infectivity assessed by counting GFP-positive cells 24 hpi (I, K, and L) and by viral yield assay 72 hpi (J), other conditions same as B. (**M**) The potential cytotoxicity of VPD exposure for 24 and 72 hours was assessed in uninfected mouse fibroblasts by the red fluorescent EthD-1 assay. The effect of VPD at 1 and 10 mM on NIH/3T3 was compared with vehicle (VEH) at the same concentrations and plain media. (**N** and **O**) The EthD-1 assay was performed to evaluate VPD protective role on viral-mediated cytotoxicity. Images show red fluorescent photomicrographs of NIH/3T3 cells pre-treated with VPD or vehicle at 10 mM for 24 hrs prior to viral inoculation (MOI of 0.03). 72 hpi, EthD-1 was added to cells. After 20 minutes, photos were captured (N) and red fluorescent-labeled cells were counted (O). Scale bar 50 μm. Mean ± SEM of 8 (C, D, G, H, M, and O) and 6 (I to L) cultures; ns, not significant, * $p < 0.05$, ** $p < 0.01$, *** $p < 0.001$, **** $p < 0.0001$, as compared to control, ANOVA with Bonferroni's post-hoc test.

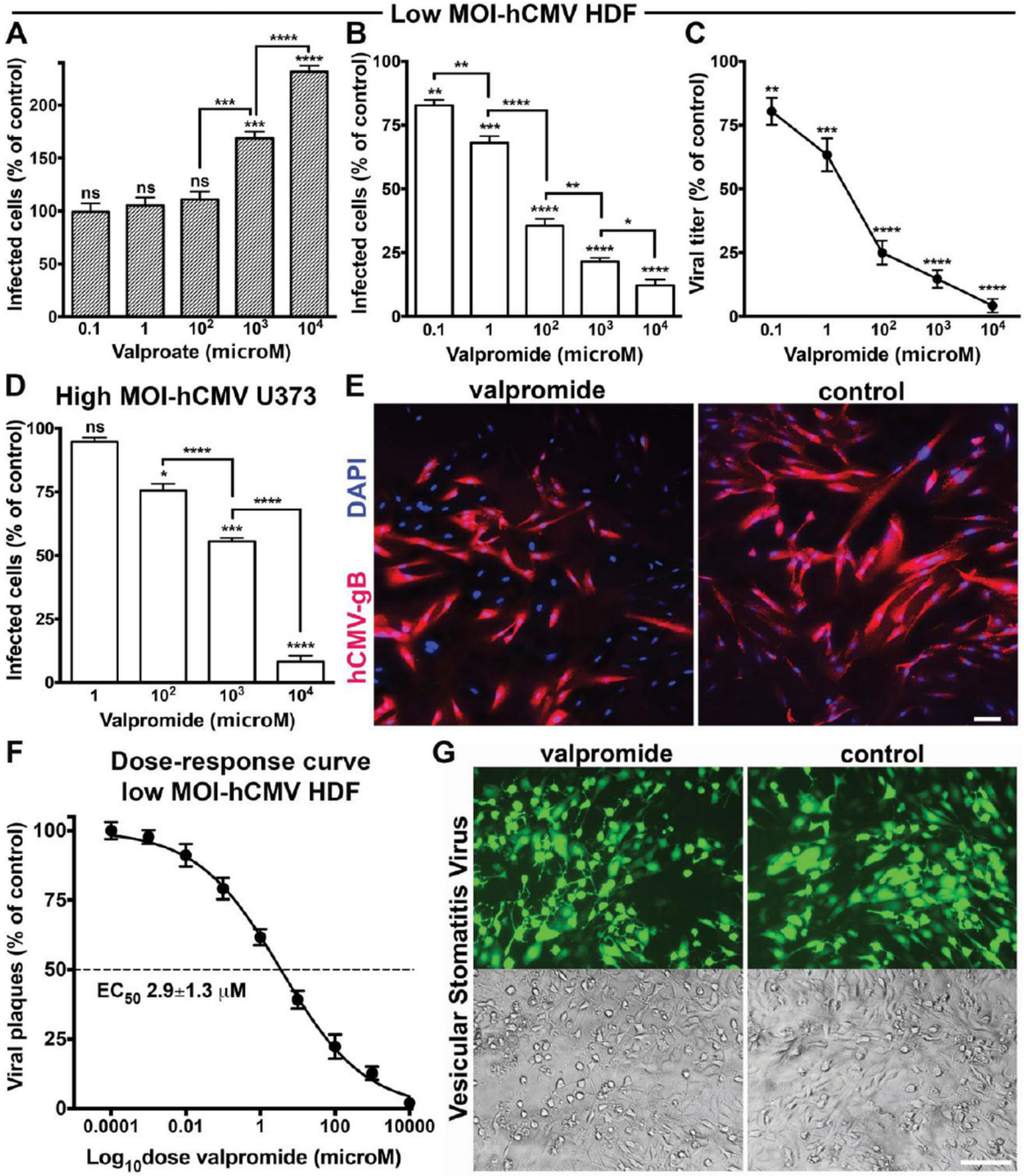

Fig. 2. Valpromide inhibits human CMV but has no effect on vesicular stomatitis virus infection

(**A**) Normal human dermal fibroblasts (HDF) were treated with VPA or vehicle at the indicated concentrations for 24 hrs prior to hCMV-GFP inoculation (MOI 0.01). Results collected at 72 hpi. (**B** and **C**) VPD dose-dependent decrease in hCMV infection assessed by counting infected GFP-positive cells at 72 hpi (B) and viral yield assay at 96 hpi (C); other conditions same as A. (**D**) Pre-treated human glioblastoma cells infected with hCMV-GFP at high titer (MOI 4). GFP-positive cells counted at 48 hpi; other conditions same as A. Data presented as mean ± SEM of 8 cultures (A to C) and 6 cultures (D); ns, not significant, * p <

0.05, ** $p < 0.01$, *** $p < 0.001$, **** $p < 0.0001$, one-way ANOVA (Bonferroni's post-hoc test). (**E**) Immunostaining for hCMV gB was done to exclude a potential inhibitory effect of VPD on GFP expression. HDF were exposed to VPD or vehicle (1 mM) for 24 hrs prior to viral challenge (MOI 1). Representative fields with hCMV gB immunoreactivity in red and cell nuclei in blue (DAPI) show VPD-mediated decrease in the relative number of infected cells. Scale bar 50 μm. (**F**) HDF cells pre-treated with VPD for 24 hours and infected with hCMV-GFP (MOI 0.01) were incubated for 7 days before viral fluorescent plaques counting. The mean plaque count for each drug concentration was expressed as a percentage of the control (vehicle) and plotted as a function of the drug dose in logaritmic scale. The concentration producing 50% reduction in plaque formation (EC_{50}) is shown. Mean ± SEM of 2 independent experiments. (**G**) Images of representative microscopic fields under GFP fluorescence (top) and phase contrast (bottom) of Vero cells pre-treated with VPD or vehicle at 1 mM for 24 hrs and infected with VSV-GFP (MOI 0.001). No drug-mediated inhibitory effect was identified (101% ± 5%, compared to control; mean ± SEM of 6 cultures). Photos captured at 24 hpi; scale bar 50 μm.

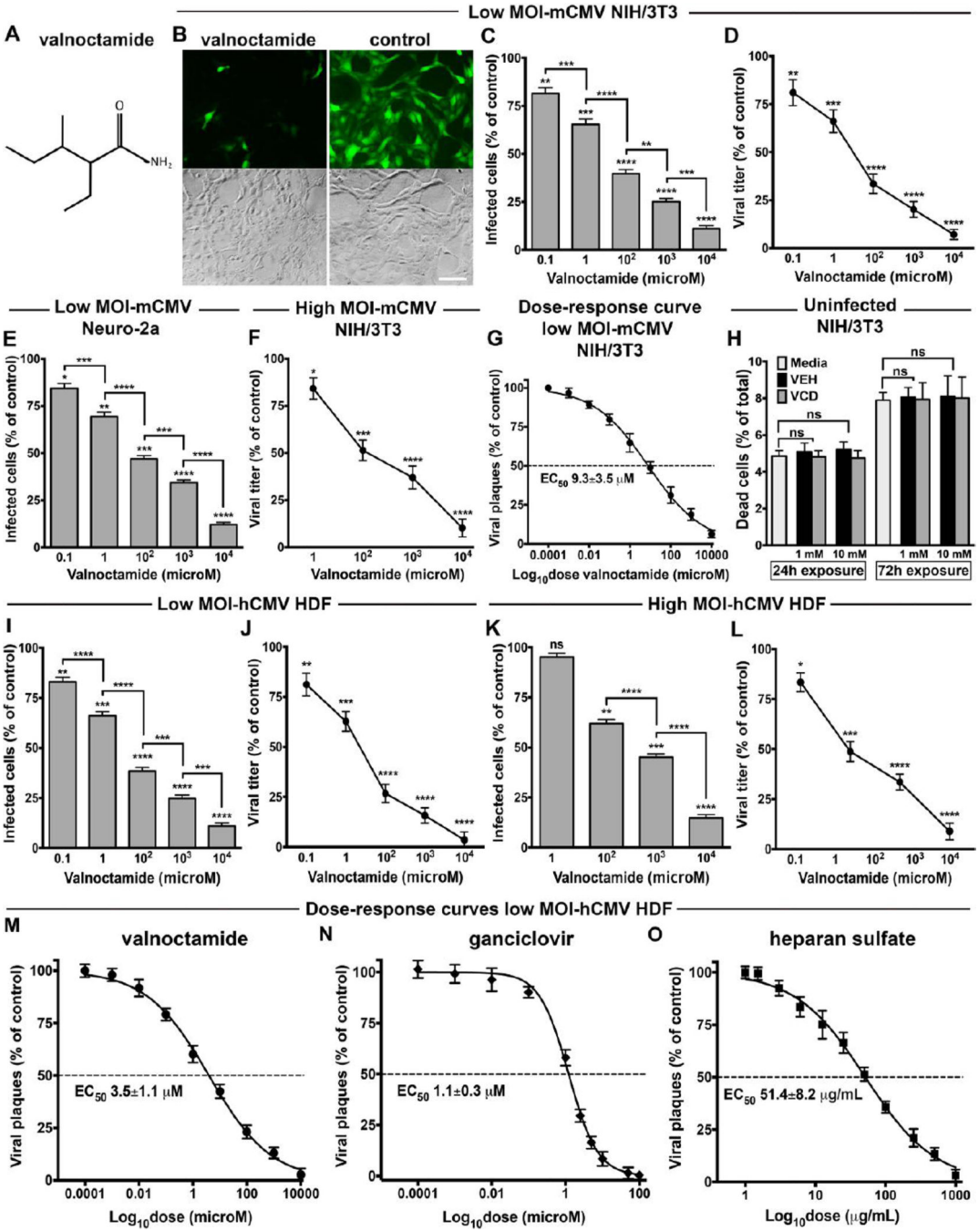

Fig. 3. Valnoctamide blocks mouse and human CMV

(**A**) Chemical structure of valnoctamide. (**B**) Microscopic fields show GFP fluorescence (top) and phase contrast (bottom) of NIH/3T3 cells pre-treated (24hrs) with VCD (1mM) or vehicle prior to inoculation with mCMV (MOI 0.03). Photos captured 48 hpi; scale 50 μm. (**C** to **F**) VCD-mediated dose-dependent decrease in mCMV infection at low MOI (0.03, C to E) and high MOI (4, F) in NIH/3T3 cells (C, D, and F) and neuro-2a (E) as assessed by counting infected GFP-positive cells at 48 hpi (C to E) and viral yield assay at 72 hpi (F); other conditions same as B. (**G**) Dose-response analysis in NIH/3T3 cells pre-treated with

VCD for 24 hours, infected with mCMV-GFP (MOI 0.03), and incubated for 4 days before viral fluorescent plaques counting. The EC_{50} is shown. Mean ± SEM of 2 independent experiments. (**H**) The potential cytotoxic effect of VCD at 1 and 10 mM on uninfected NIH/3T3 after 24 and 72 hours of exposure was assessed by the red fluorescent EthD-1 assay and results compared with vehicle (VEH) at the same concentrations and plain media. (**I** to **L**) VCD-mediated decrease in hCMV infection at low MOI (0.01, I and J) and high MOI (1, K and L) in human dermal fibroblasts, evaluated by GFP-positive cells counting at 48 hpi (K) or 72 hpi (I) and viral yield assay at 96 hpi (J and L). Mean ± SEM of 8 (C to E, and H to J) and 6 (F, K, and L) cultures; ns, not significant, * $p < 0.05$, ** $p < 0.01$, *** $p < 0.001$, **** $p < 0.0001$, one-way ANOVA (Bonferroni's post-hoc test). (**M** to **O**) Dose-response analysis by plaque reduction assay in HDF cells pre-treated with VCD (M), GCV (N), or HS (O) for 24 hours and infected with hCMV-GFP (MOI 0.01). Viral fluorescent plaques counting at 7 dpi. Mean ± SEM of 2 independent experiments.

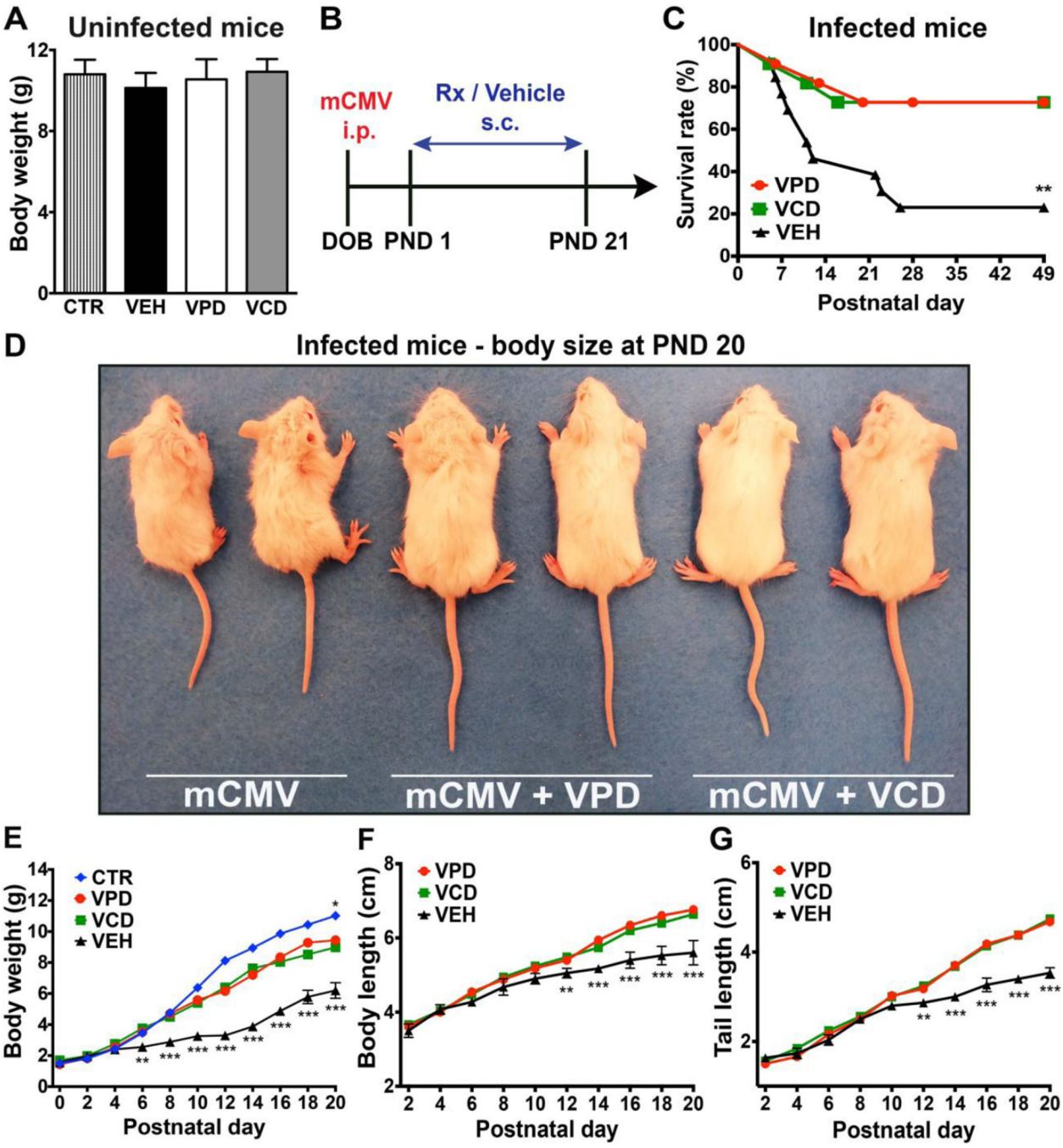

Fig. 4. Valpromide and valnoctamide safely improve survival and postnatal body growth of infected newborns

(**A**) Uninfected pups received 20 μL of saline (CTR), vehicle (VEH), VPD, or VCD (1.4 mg/mL), once a day, subcutaneously, from PND 1 to PND 21, when the body weight was assessed. Mean ± SEM, one-way ANOVA with Bonferroni's post-hoc test; N=8 mice/experimental group. (**B**) Timeline showing mCMV infection of neonates and compounds administration. (**C**) Survival at PND 49 assessed by Log-rank (Mantel-Cox) test; N=11–13 mice/group. (**D** to **G**) Drug-induced improvement in postnatal body growth. Photo shows

enhanced body size of VPD- and VCD-treated pups compared to vehicle (mCMV) (D). Graphs show postnatal body weight (E), body length (F), and tail length (G) increase from DOB to PND 20. CTR, control/uninfected mice treated with saline; VPD, VCD, and VEH, infected newborns treated with the indicated compounds. Mean ± SEM; error bars shown for VEH group; N=6–9 mice/group; mixed-model ANOVA (Newman Keuls test) for VPD and VCD versus CTR (E) and for VPD and VCD versus VEH (E to G); * $p < 0.05$, ** $p < 0.01$, *** $p < 0.001$.

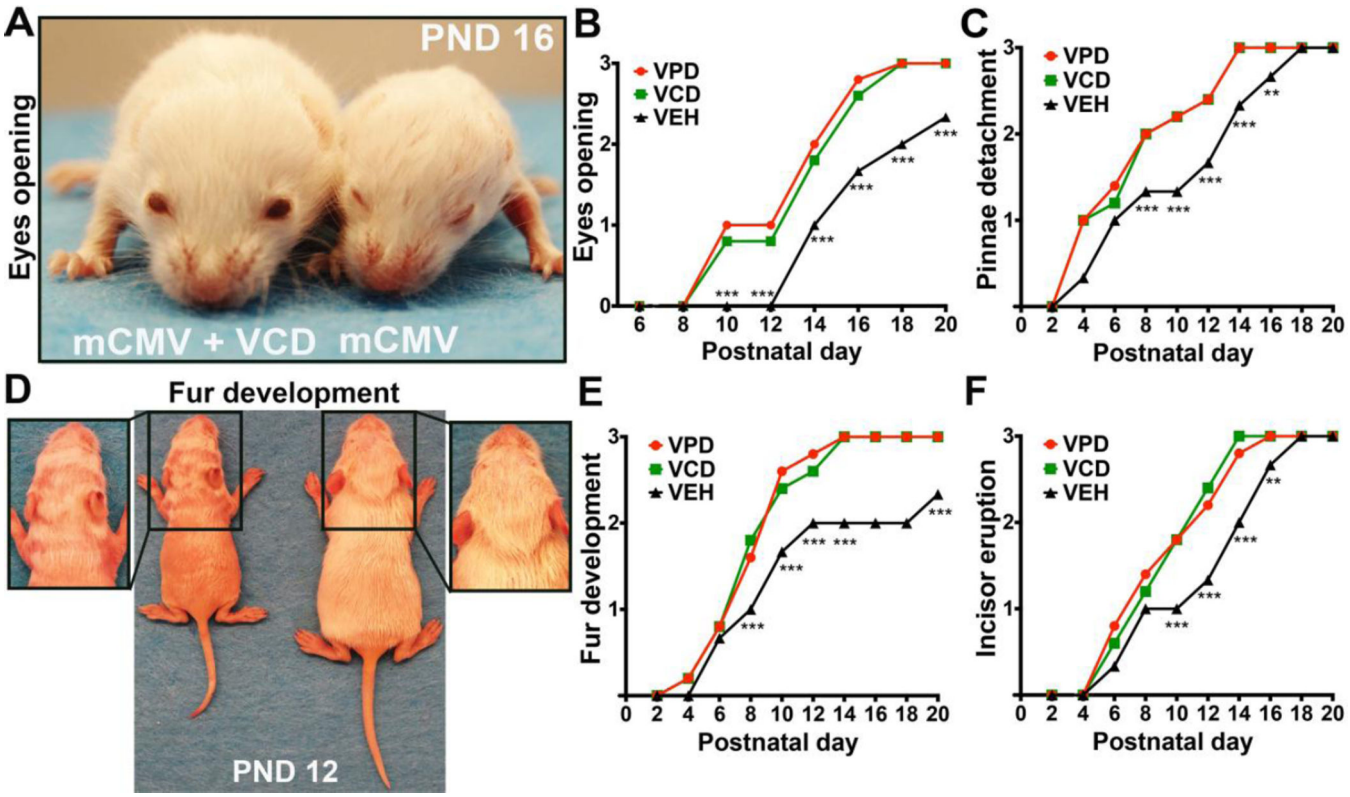

Fig. 5. Daily valpromide and valnoctamide administration ameliorates postnatal somatic development

(**A** to **F**) Graphs show progressive improvement of multiple parameters of postnatal growth. Mean ± SEM; error bars not shown for clarity. N=6–9 mice/group; mixed-model ANOVA (Newman Keuls test) for VPD and VCD versus VEH; ** $p < 0.01$, *** $p < 0.001$. Photos show the differential status of eyes opening (A) and the delayed development of fur in an infected/untreated pup (left) compared to an infected newborn treated with VCD (right) (D); marked difference in growth is also evident.

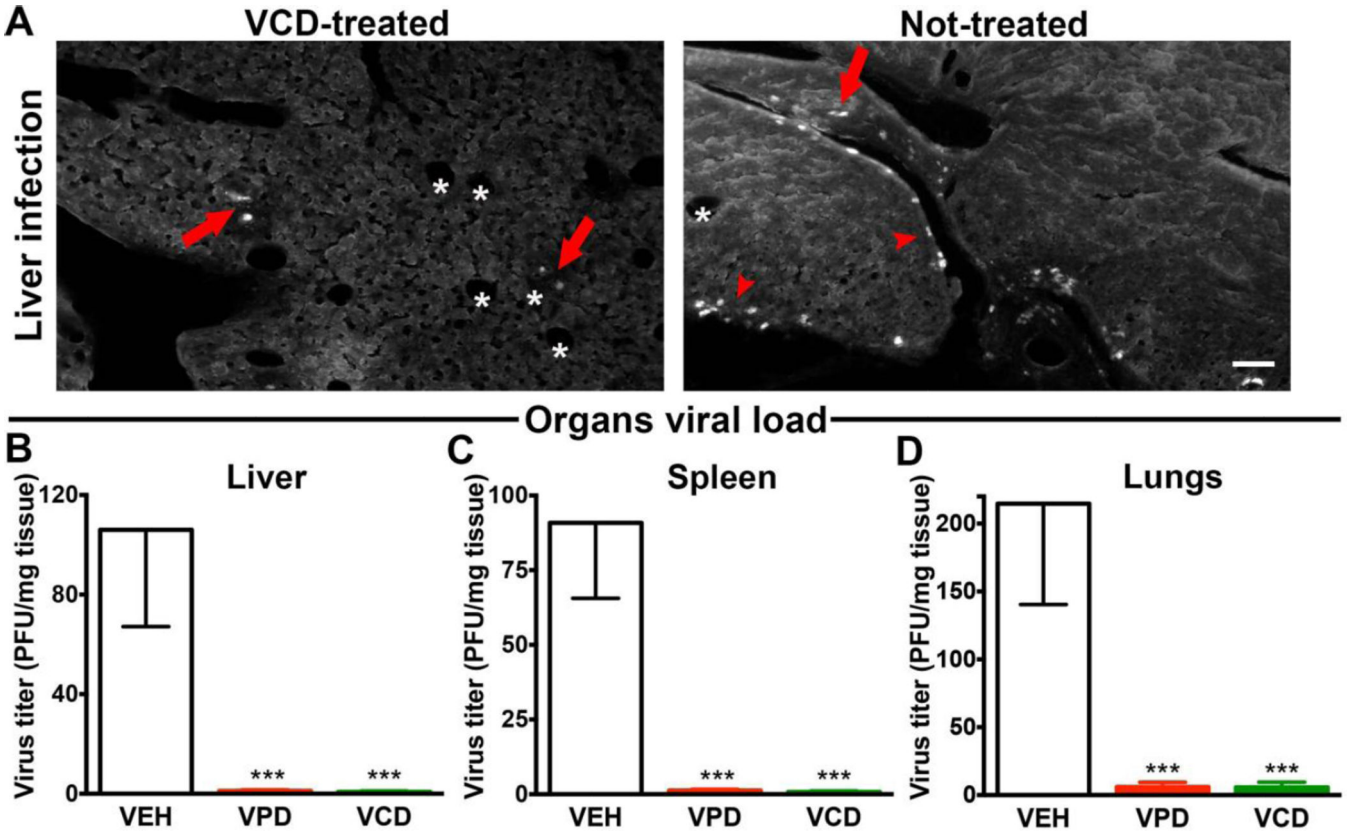

Fig. 6. Valpromide and valnoctamide substantially decrease CMV load in target organs

(**A**) A small number of cells show CMV infection in the liver of PND 12 mice infected on DOB and treated daily with VCD until PND 10 (left); in contrast, a higher number was commonly found in the liver of pups receiving vehicle (right). GFP-positive cells are localized both in the parenchyma (arrows) and in the sub-peritoneal area (arrowheads). Asterisks indicate lobule central veins. Scale 100 μm. (**B** to **D**) Infected newborns treated with VPD, VCD, or VEH from PND 1 to 10, were euthanized at PND 12, and tissue samples from liver, spleen, and lungs were collected for measurement of viral titer by plaque assay. Bar graphs show titers as PFU/mg of tissue; mean ± SEM; N=6 mice/group; *** $p < 0.001$, one-way ANOVA, Bonferroni's post-hoc test.

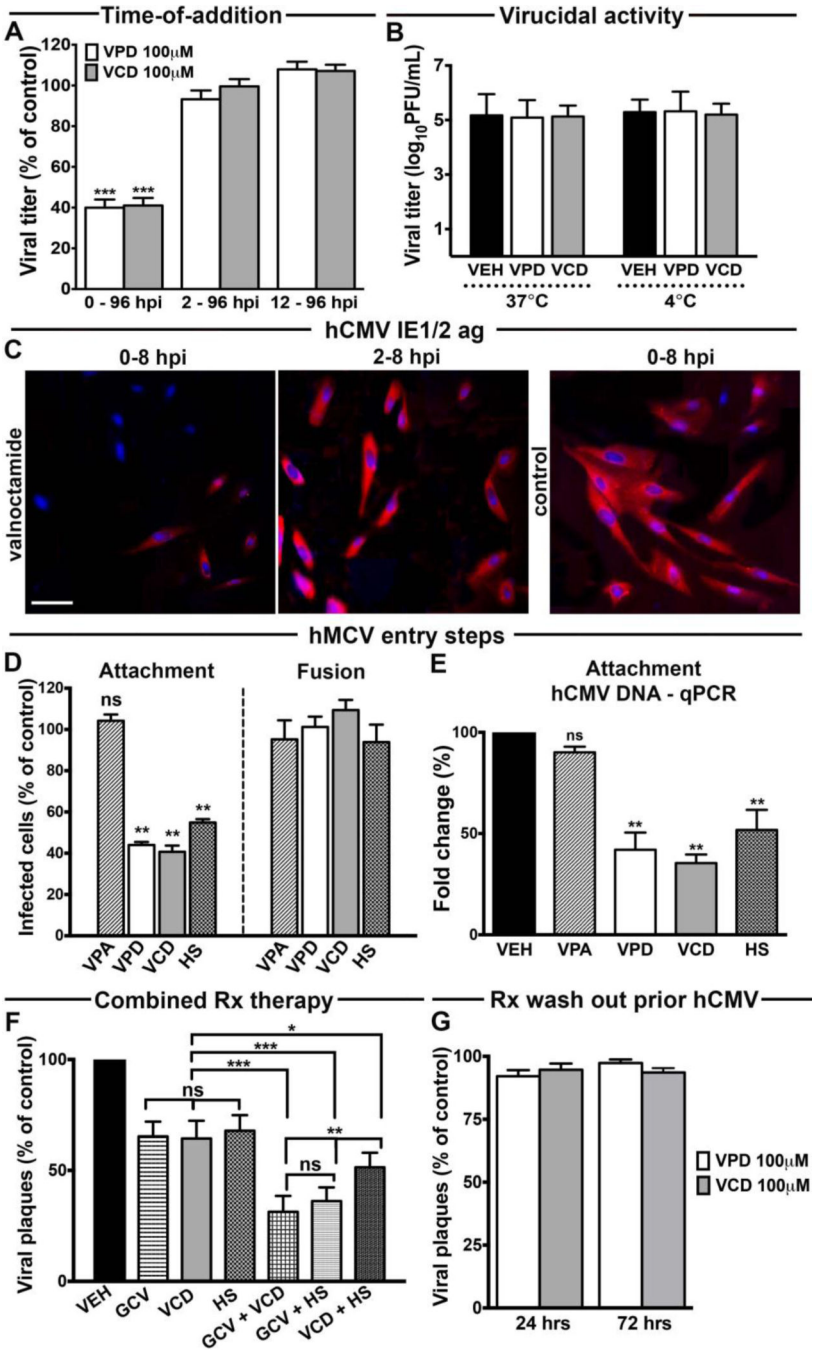

Fig. 7. Valpromide and valnoctamide inhibit hCMV attachment to cell

(**A**). HDF cells infected with hCMV-GFP (MOI 0.01) (t=0) were exposed to VPD, VCD, or vehicle (100 μM) simultaneously, or 2 or 12 hours after virus inoculation until media collection at 96 hpi. Viral replication assessed by titer determination using a plaque assay on HDF monolayers. (**B**) A drug (100 μM)/undiluted hCMV mixture was incubated for 2 hours at 37°C or 4°C. Before cell inoculation, the solution was diluted to 10 nM (ineffective drug concentration). (**C**) Human fibroblasts infected with hCMV (MOI 0.01) and treated with the compounds (100 μM) starting from viral challenge (t=0) or 2 hpi, were fixed and

permeabilized at 8 hpi for immunofluorescence with anti-IE1/2 monoclonal antibody and DAPI staining. Scale bar 100 μm. (**D** and **E**) Attachment and fusion assays were performed as described in Materials and Methods. GFP-positive cells were counted at 72 hpi (D). Results presented as the fold change ($2^{-\Delta\Delta CT}$) of hCMV DNA in each experimental condition relative to vehicle (mean ± SEM of 2 biological replicates) (E). (**F**) Plaque reduction assay on HDF cells exposed to vehicle, GCV (100 nM), VCD (1 μM), HS (25 μg/mL – 40 μM), or a combination of these compounds as indicated for 24 hours before hCMV inoculation (MOI 0.01). Fluorescent plaques counted at 7 dpi. The mean plaque counts for each drug were expressed as a percentage of the control (vehicle) mean plaque count, defined as 100%; $p < 0.001$ for VEH vs GCV, VCD, and HS. Rx, drug. (**G**) After 24 hrs-or 72 hrs-VPD, VCD, or vehicle pre-treatment (100 μM), cultures were rinsed three times and given drug-free media prior to hCMV inoculation (MOI 0.01). Plaques counted at 7 dpi. Bars: mean ± SEM of 5 (F and G), 8 (A and B), and 12 cultures (D); ns, not significant, * $p < 0.05$, ** $p < 0.01$, *** $p < 0.001$, one-way ANOVA with Bonferroni's post-hoc test.

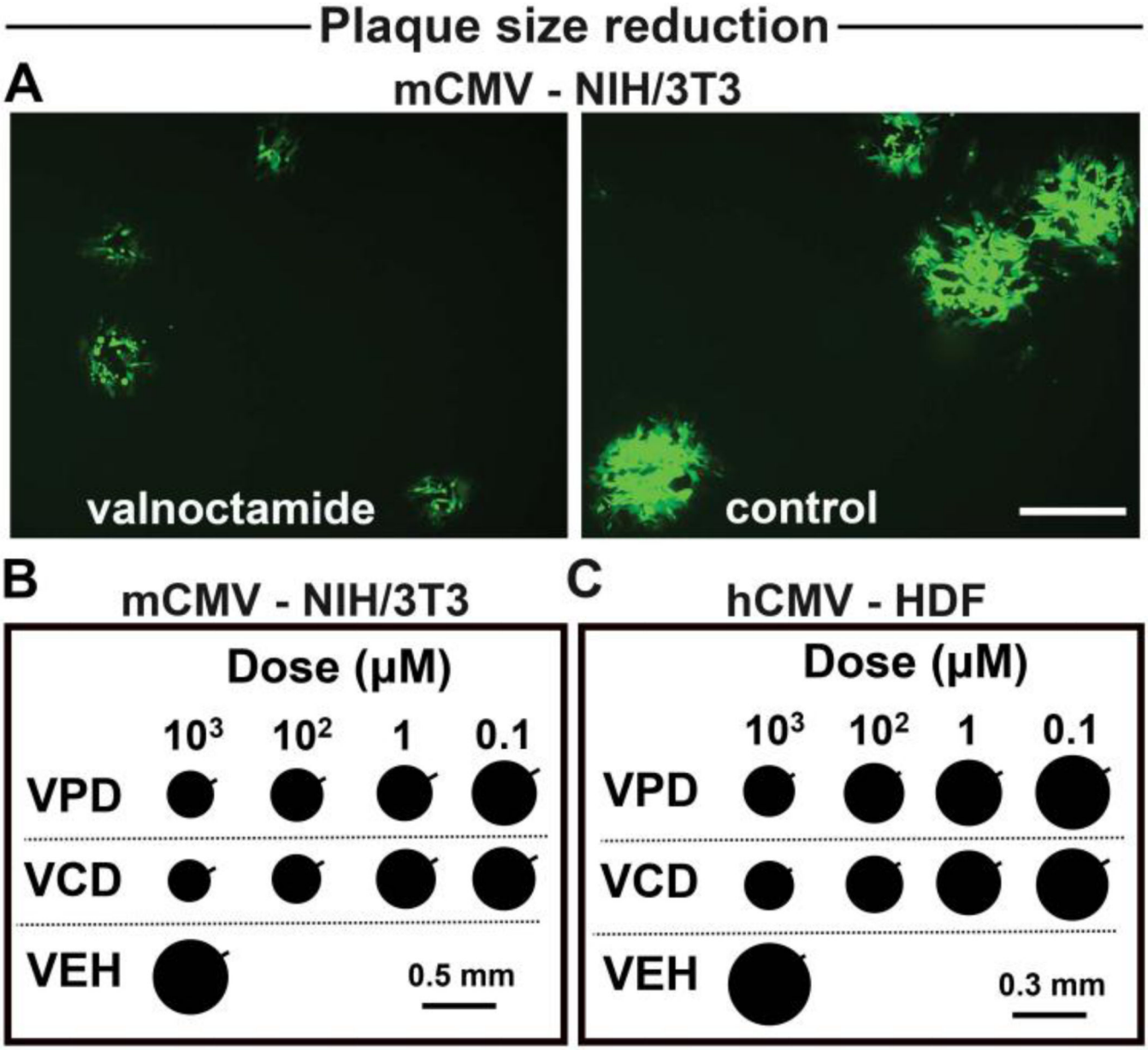

Fig. 8. Valpromide and valnoctamide effectively decrease spread of CMV infection

(**A** to **C**) Plaque size assay of NIH/3T3 cells (A and B) and human fibroblasts (C) infected with mCMV-GFP and hCMV-GFP (MOI 1) and treated with VPD, VCD, or vehicle. Viral plaque size measured 5 (mCMV) and 10 (hCMV) dpi. Representative plaques in 100 μM VCD (left) or vehicle (right); scale 300 μm (A). Mean diameter of 60 random plaques; $p < 0.05$ in 0.1 μM, $p < 0.01$ in 1 μM, $p < 0.001$ in 100 μM and 1 mM, versus vehicle. SEM, bar on upper right side (B and C).